PREPRINT
IN-71
© WAIVED
AVAIL: CASI

AIAA 2000-0345

Modeling Aerodynamically Generated Sound:

Recent Advances in Rotor Noise Prediction

Kenneth S. Brentner
NASA Langley Research Center
Hampton, Virginia

38th Aerospace Sciences Meeting & Exhibit
10 – 13 January 2000 / Reno, NV

MODELING AERODYNAMICALLY GENERATED SOUND: Recent Advances in Rotor Noise Prediction

Kenneth S. Brentner*
NASA Langley Research Center
Hampton, Virginia

Abstract

A great deal of progress has been made in the modeling of aerodynamically generated sound for rotors over the past decade. The Ffowcs Williams–Hawkings (FW–H) equation has been the foundation for much of the development. Both subsonic and supersonic quadrupole noise formulations have been developed for the prediction of high-speed impulsive noise. In an effort to eliminate the need to compute the quadrupole contribution, the FW–H has also been utilized on permeable surfaces surrounding all physical noise sources. Comparison of the Kirchhoff formulation for moving surfaces with the FW–H equation have shown that the Kirchhoff formulation for moving surfaces can give erroneous results for aeroacoustic problems.

1. Introduction

Noise has been an undesirable byproduct of aerospace vehicles from the time of early aircraft until now. Originally, aircraft noise was not much of an issue because of the overarching requirement of improving vehicle performance. As aerospace technology has matured, more resources have been devoted to the reduction of aerodynamically generated sound. With the maturation of the aerospace technology already achieved, both the public and regulatory bodies have focused their concern on safety, emissions, and noise rather than either performance or efficiency. This situation is really a credit to the success of past generations of aerospace designers and engineers. The challenge now facing us is that anticipated increases in the utilization of air travel will also bring unacceptable increases in aircraft noise—if nothing is done. Fortunately, a great deal of progress has been made both in understanding the noise-generation mechanisms and in developing first-principles models for prediction of the sound.

Rotorcraft are inherently complex aeromechanical vehicles, and hence have lagged fixed-wing aircraft in the understanding of the mechanisms responsible for rotor noise and accurate and efficient prediction methods based upon the fluid physics (as opposed to empirical methods). A number of high quality experimental tests, concentrated national programs and rigorous theoretical developments have greatly expanded both our understanding of rotor noise sources and our ability to predict rotor noise. The maturation of computational fluid dynamics (CFD) and its application to rotor aerodynamics has been an enabling step necessary for accurate, first-principles noise prediction. Nevertheless, rotor aerodynamics is often one of the weak links leading to unsatisfactory acoustic computations.

In this paper, the focus will be on the aerodynamically generated sound of rotors and the recent advances in rotor noise prediction. In 1994, Brentner and Farassat published a status report on helicopter noise prediction. Their report provides a historical perspective and method assessment that is a useful backdrop for this paper. A significant body of work has been completed since 1994, therefore, it is the intent of this paper to put both theoretical and computational developments in perspective. This paper places some emphasis on theoretical development and interpretation because these always help explain the reason various computational methods were chosen. Advances in source noise prediction are the primary focus of this paper even though system noise prediction is recognized as an important area that still lacks sufficient capabilities.

2. Theoretical Background: FW–H equation

The problem of aerodynamically generated sound is governed by the conservation laws of mass, momentum and energy. The FW–H equation[1] is an exact rearrangement of the continuity equation and the Navier–Stokes equations into the form of an in-

*Senior Research Engineer, Computational Modeling and Simulation Branch, Senior Member AIAA.

homogeneous wave equation with two surface source terms and a volume source term. The FW–H equation is the most general form of the Lighthill acoustic analogy[2] and is appropriate for predicting the noise generated by the complex motion of helicopter rotors. Today almost all deterministic rotor noise predictions are based on time-domain integral formulations of the FW–H equation. In this section, the FW–H equation will be examined to provide the background necessary to understand the recent advances in rotor noise prediction. The close relationship between the FW–H equation and the Kirchhoff formulation for moving surfaces will be discussed later.

2.1 Derivation

The FW–H equation may be derived by embedding the exterior flow problem in unbounded space by using generalized functions to describe the flow field. To do this, consider a moving surface $f(\mathbf{x},t)=0$ with a stationary fluid outside. The surface $f=0$ is defined such that $\nabla f = \hat{\mathbf{n}}$, where $\hat{\mathbf{n}}$ is a unit normal vector pointing toward the exterior of the surface. Inside $f=0$ the generalized flow variables are defined to have their freestream values, i.e.,

$$\tilde{\rho} = \rho' H(f) + \rho_o \tag{1}$$

$$\widetilde{\rho u_i} = \rho u_i H(f) \tag{2}$$

and

$$\tilde{P}_{ij} = P'_{ij} H(f) + p_o \delta_{ij} \tag{3}$$

where the tilde indicates that the variable is a generalized function defined throughout all space. On the right hand side ρ, ρu_i, and P_{ij} are the density, momentum, and compressive stress tensor, respectively. Freestream quantities are indicated by the subscript o, primed quantities represent the difference from the freestream value (e.g., $\rho' = \rho - \rho_o$), δ_{ij} is the Kronecker delta and $H(f)$ is the Heaviside function. (Note: for an inviscid fluid, $P_{ij} = p\delta_{ij}$.)

Substituting the generalized density and momentum definitions (1)–(2) into the continuity equation and collecting the derivatives of the Heaviside function on the right-hand side yields a generalized continuity equation written as

$$\frac{\bar{\partial}\tilde{\rho}}{\partial t} + \frac{\bar{\partial}\widetilde{\rho u_i}}{\partial x_i} = (\rho' \frac{\partial f}{\partial t} + \rho u_i \frac{\partial f}{\partial x_i})\delta(f) \tag{4}$$

Here the bar over the derivative operators indicate that generalized differentiation (i.e., differentiation of generalized functions) is implied. Also note that $\partial f/\partial t = -v_n$, $\partial f/\partial x_i = \hat{n}_i$ and $\partial H(f)/\partial f = \delta(f)$ is the Dirac delta function. This generalized continuity equation is valid for the entire space—both inside and outside of the body. The generalized momentum equation can be written

$$\frac{\bar{\partial}\widetilde{\rho u_i}}{\partial t} + \frac{\bar{\partial}\widetilde{\rho u_i u_j}}{\partial x_j} + \frac{\bar{\partial}\tilde{P}_{ij}}{\partial x_j} = (\rho u_i \frac{\partial f}{\partial t} + (\rho u_i u_j + P'_{ij})\frac{\partial f}{\partial x_j})\delta(f) \; . \tag{5}$$

Now by taking the time derivative of equation (4) and subtracting the divergence of equation (5), followed with some rearranging, the FW–H equation may be written as the following inhomogeneous wave equation:

$$\begin{aligned}\Box^2 c^2 \rho'(\mathbf{x},t) = {} & \frac{\bar{\partial}^2}{\partial x_i \partial x_j}[T_{ij} H(f)] \\ & - \frac{\partial}{\partial x_i}[(P'_{ij}\hat{n}_j + \rho u_i (u_n - v_n))\delta(f)] \\ & + \frac{\partial}{\partial t}[(\rho_o v_n + \rho(u_n - v_n))\delta(f)]\end{aligned} \tag{6}$$

where T_{ij} is the Lighthill stess tensor, u_n is the fluid velocity in the direction normal to the surface $f=0$ and v_n is the surface velocity in the direction normal to the surface. On the left hand side we use the notation $\Box^2 = [(1/c^2)(\partial^2/\partial t^2)] - \nabla^2$.

If the fictitious surface $f=0$ coincides with a solid surface, then the normal velocity of the fluid is the same as the normal velocity of the surface ($u_n = v_n$). Then equation (6) can be written

$$\begin{aligned}\Box^2 p'(\mathbf{x},t) = {} & \frac{\bar{\partial}^2}{\partial x_i \partial x_j}[T_{ij} H(f)] \\ & - \frac{\partial}{\partial x_i}[(P'_{ij}\hat{n}_j \delta(f)] + \frac{\partial}{\partial t}[(\rho_o v_n)\delta(f)]\end{aligned} \tag{7}$$

where on the left hand side we use the customary notation $p' \equiv c^2\rho'$ because the observer location is outside of the source region.

2.2 Interpretation

The three source terms on the right-hand side of equation (7) are known as the thickness, loading, and quadrupole source terms, respectively. A formal solution may be obtained by using the free-space Green's function and utilizing the fact that the FW–H equation is valid in the entire unbounded space.

Note in equation (7) that the thickness and loading source terms are surface distributions of sources (indicated by the presence of the Dirac delta function $\delta(f)$). The thickness source accounts for the noise generated by the displacement of fluid as the body passes while the loading source term accounts for noise that results from the unsteady motion of the force distribution on the body surface. The thickness and loading source terms have been used for several years in rotor noise prediction because they account for most of the acoustic signal when the flow field is not transonic. Furthermore, they do not require knowledge of the flow field off the blade (although the accurate determination of the blade-surface pressure is still challenging).

The quadrupole source, on the other hand, is a volume distribution of sources (indicated by the Heaviside function $H(f)$). The quadrupole source accounts for the nonlinearities due to both the local sound speed variation and the finite particle velocity near the blade. The importance of the quadrupole term has long been recognized,[3,4] however, the quadrupole source has often been neglected in rotor noise prediction because of the computational demands of computing the flow field with sufficient accuracy and integrating over a volume in the acoustic prediction.

It is interesting to note that the form of the various source terms is not unique.[5] One example of this, known as Isom thickness noise, is that the thickness source term in equation (7) is equivalent to a constant pressure $c^2\rho_o$ over the body in the loading source term.[6] Although mathematically equivalent, the two formulations for thickness noise have quite different characteristics and robustness when integrated numerically. Much of the recent work on the FW–H equation has been connected with efficient evaluation of the quadrupole source term or development of a more numerically suitable, but equivalent source description.

2.3 Integral Formulations

A key feature of the FW–H equation is that it is an inhomogeneous wave equation for the external flow problem that has been embedded in unbounded space. Hence, an integral representation of the solution can be readily found using the free-space Green's function. The particular formulation that is developed results primarily from the choice of the change of variables needed to analytically integrate the Dirac delta functions.

To illustrate, we consider the following example. An inhomogeneous wave equation can be written as

$$\Box^2\phi(\mathbf{x},t) = Q(\mathbf{x},t)\delta(f) \tag{8}$$

where $Q(\mathbf{x},t)$ is the source strength. Equation (8) is typical of the various surface-source terms in the FW–H equation. By using the free-space Green's function $\delta(g)/4\pi r$, an integral representation of the solution may be written as

$$4\pi\phi(\mathbf{x},t) = \int_{-\infty}^{t}\int_{-\infty}^{\infty} \frac{Q(\mathbf{y},\tau)\delta(f)\delta(g)}{r} d\mathbf{y}d\tau\ . \tag{9}$$

The next stage in developing the acoustic formulation is to integrate the Dirac delta functions $\delta(f)$ and $\delta(g)$, a process that requires a change of variables. This change of variables determines the type of formulation. Equation (9) can be expressed as

$$\begin{aligned} 4\pi\phi(\mathbf{x},t) &= \int_{f=0} \left[\frac{Q(\mathbf{y},\tau)}{r|1-M_r|}\right]_{ret} dS && (10) \\ &= \int_{-\infty}^{t} \int_{\substack{f=0 \\ g=0}} \frac{Q(\mathbf{y},\tau)}{r\sin\theta} c d\Gamma d\tau && (11) \\ &= \int_{F=0} \frac{1}{r}\left[\frac{Q(\mathbf{y},\tau)}{\Lambda}\right]_{ret} d\Sigma && (12) \end{aligned}$$

with the variable transformations $(\tau, y_3) \rightarrow (g, f)$, $(y_2, y_3) \rightarrow (f, g)$, and $(\tau, y_3) \rightarrow (g, F)$, respectively. (See reference 7 for definitions.) The three formulations expressed in equations (10)–(12) will be termed retarded-time, collapsing-sphere, and emission-surface formulations, respectively. Each type of formulation has its own physical and geometrical interpretation. For volume source terms, such as the quadrupole, only retarded-time and collapsing-sphere formulations are found.

3. Recent Advances

Now that the ground work has been laid, it is time to consider some of the recent advances in rotor noise prediction. This presentation focuses primarily on formulation development and implementation at NASA Langley during the 1990's.

3.1 High-Speed Impulsive Noise

High-speed impulsive (HSI) noise is a particularly intense and annoying noise generated by helicopter rotors in high-speed forward flight. HSI noise is closely associated with the appearance of shocks and transonic flow around the advancing rotor blades and is accounted for by the FW–H quadrupole source. Farassat and Brentner[8] have shown that after some manipulation of the formal solution the noise contribution from the quadrupole may be expressed as

$$4\pi p'_Q(\mathbf{x},t) = \frac{1}{c}\frac{\partial^2}{\partial t^2}\int_{-\infty}^{t}\int_{f>0}\frac{T_{rr}}{r}d\Omega d\tau + \frac{\partial}{\partial t}\int_{-\infty}^{t}\int_{f>0}\frac{3T_{rr}-T_{ii}}{r^2}d\Omega d\tau + c\int_{-\infty}^{t}\int_{f>0}\frac{3T_{rr}-T_{ii}}{r^3}d\Omega d\tau \quad (13)$$

where $p'_Q(\mathbf{x},t)$ is the acoustic pressure due to the quadrupole source. The quantity T_{rr} is the double contraction of the Lighthill stress tensor T_{ij} with $\hat{r}_i$ and $\hat{r}_j$; where $\hat{r}_i$ are the components of the unit vector in the radiation direction. In addition, $d\Omega$ is an element of the surface $g=0$, which is known as the collapsing sphere; hence, equation (13) is known as the collapsing sphere formulation. Equation (13) is interpreted as an inner integration over the sphere of radius $r=c(t-\tau)$ centered at the observer. The outer integration of $-\infty<\tau\leq t$ sums the contribution from all spheres.

An integration over the entire collapsing sphere surface is not actually necessary in the inner integrals of equation (13) because the Lighthill stress tensor T_{ij} vanishes away from the source region. For an in-plane observer in the far field, the collapsing sphere can be locally approximated by a right circular cylinder, as shown in figure 1. Because the observer is assumed to be in the rotor plane (precisely where HSI noise has maximum directivity), integration in the normal direction to the rotor plane can be done independent of the observer position. Yu et al.[3] were the first to use this far-field approximation for the evaluation of quadrupole noise; however, several additional approximations were made to both the quadrupole source strength and the acoustic integrals. These additional approximations are no longer necessary.

In the work of Brentner and Holland,[9] the integration over the approximate collapsing sphere surface is carried out in two parts. First, integration in the direction normal to the rotor disk is performed. They define the quadrupole source strength on the rotor plane as

$$Q_{ij}=\int_{f>0}T_{ij}dz \quad (14)$$

where z is understood to be in the direction normal to the rotor disk and the z integration is only done outside of the rotor blade; Q_{ij} is nonzero only over a region near the rotor blade planform, and extends ahead of the leading edge, behind the trailing edge, and off the blade tip. By using relation (14), equation (13) may now be written as

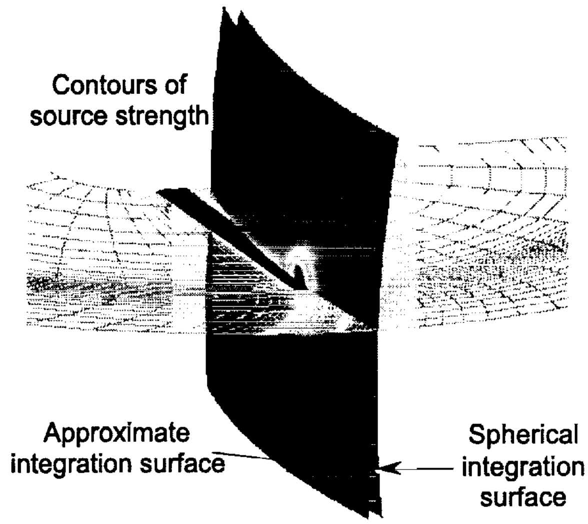

Figure 1. Far-field approximation of the collapsing sphere. Although not shown, the observer is three rotor radii to the right of the rotor blade.

$$4\pi p'_Q(\mathbf{x},t) = \frac{1}{c}\frac{\partial^2}{\partial t^2}\int_{-\infty}^{t}\int_{\substack{f^+=0\\g=0}}\frac{Q_{rr}}{r}d\Gamma d\tau + \frac{\partial}{\partial t}\int_{-\infty}^{t}\int_{\substack{f^+=0\\g=0}}\frac{3Q_{rr}-Q_{ii}}{r^2}d\Gamma d\tau + c\int_{-\infty}^{t}\int_{\substack{f^+=0\\g=0}}\frac{3Q_{rr}-Q_{ii}}{r^3}d\Gamma d\tau \quad (15)$$

where $f^+=0$ represents the rotor-disk plane. The intersection of the collapsing sphere with the rotor plane results in a curve for which we use the notation Γ.

3.1.1 Subsonic Formulation

In the development of a subsonic quadrupole formulation, equation (15) is transformed from a collapsing sphere formulation to a retarded-time formulation (as was discussed previously). When the time derivatives are taken inside the retarded-time integrals,[10] the quadrupole formulation may be written

$$4\pi p'_Q(\mathbf{x},t) = \int\limits_{f^+=0} \left[\frac{K_{r1}}{c^2 r} + \frac{K_{r2}}{c r^2} + \frac{K_{r3}}{r^3}\right]_{ret} dS \quad (16)$$

where

$$\begin{aligned} K_{r1} &= \frac{\ddot{Q}_{rr}}{(1-M_r)^3} + \frac{\ddot{M}_r Q_{rr} + 3\dot{M}_r \dot{Q}_{rr}}{(1-M_r)^4} \\ &+ \frac{3\dot{M}_r^2 Q_{rr}}{(1-M_r)^5} \\ K_{r2} &= \frac{-\dot{Q}_{ii}}{(1-M_r)^2} - \frac{4\dot{Q}_{Mr} + 2Q_{\dot{M}r} + \dot{M}_r Q_{ii}}{(1-M_r)^3} \\ &+ \frac{3[(1-M^2)\dot{Q}_{rr} - 2\dot{M}_r Q_{Mr} - M_i \dot{M}_i Q_{rr}]}{(1-M_r)^4} \\ &+ \frac{6\dot{M}_r(1-M^2)Q_{rr}}{(1-M_r)^5} \end{aligned}$$

and

$$\begin{aligned} K_{r3} &= \frac{2Q_{MM} - (1-M^2)Q_{ii}}{(1-M_r)^3} - \frac{6(1-M^2)Q_{Mr}}{(1-M_r)^4} \\ &+ \frac{3(1-M^2)^2 Q_{rr}}{(1-M_r)^5} \end{aligned}$$

Equation (16), together with the definitions of K_{r1}, K_{r2}, and K_{r3}, are referred to as formulation Q1A. Formulation Q1A does not require numerical time differentiation of the integrals and, as a retarded-time formulation, is well suited for subsonic source motion. Aside from the problem geometry, only the time-dependent value of Q_{ij} is required as input. Brentner[10] has implemented formulation Q1A in a new version of the WOPWOP noise prediction code[11]now called WOPWOP+. (Full details of the derivation are given in reference 10.)

To demonstrate the forward-flight capability of the WOPWOP+ code, Brentner[10] made a comparison of predicted and measured results for a four-blade swept-tip rotor tested in the Duits-Nederslandse Windtunnel (DNW). For this comparison, a microphone located in the rotor plane at a rotor azimuth of $\psi = 150°$ was utilized. The experiment is described in the report by Visintainer et al.[12]

The full potential solver FPRBVI[13] was used to compute the unsteady flow field around the rotor. The CFD solution was stored at every degree of rotor azimuth for the quadrupole source strength computation. The results of the forward-flight noise prediction are shown in figure 2. The experimental data is compared with the predicted acoustic pressure; the quadrupole contribution is also shown to indicate its relative magnitude. Although the CFD calculation used a rather coarse grid, the agreement is good.

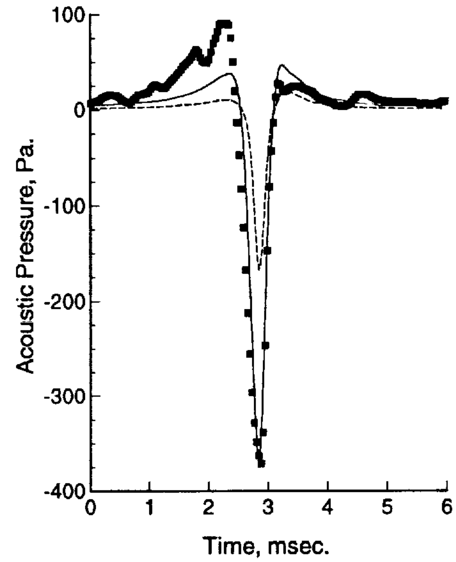

Figure 2. Contemporary design, four-blade model rotor operating in forward flight; $\mu = 0.32$ and $M_{AT} = 0.933$. ▪ experimental data; ——— predicted acoustic pressure; – – – quadrupole component of predicted acoustic pressure.

3.1.2 Supersonic Formulation

To develop a supersonic quadrupole formulation, equation (15) is transformed from a collapsing sphere formulation to an emission-surface formulation. The emission-surface formulation is appropriate for supersonic-source motion because it does not have a Doppler singularity $|1-M_r|$ in the denominator of the integrand. Farassat and Brentner[14] took the time derivatives inside the integrals by recognizing that the entire rotor plane can be considered as the emission-surface, hence the limits of integration are not a problem. Next they changed coordinates from a frame fixed to the undisturbed medium to a frame always aligned with the rotor blade, (i.e. $(\mathbf{x},t) \to (\boldsymbol{\eta},\tau)$). The effect of this operation on the tensor $\mathbf{Q}$ with components Q_{ij} is

$$\begin{aligned} \left.\frac{\partial [Q_{ij}]_{ret}}{\partial t}\right|_{\mathbf{x}} &= \left[\left.\frac{\partial}{\partial \tau}\right|_{\mathbf{x}} Q_{ij}\right]_{ret} \\ &= \left[\left.\frac{\partial Q_{ij}}{\partial \tau}\right|_{\boldsymbol{\eta}} - \mathbf{V}\cdot\nabla_{\boldsymbol{\eta}} Q_{ij}\right]_{ret} \quad (17) \\ &\equiv \left[L_\tau Q_{ij}\right]_{ret} \end{aligned}$$

where $\boldsymbol{\eta}$ is the position vector in the rotating frame and τ is the source time. Here $\mathbf{V} = \partial\boldsymbol{\eta}/\partial\tau$ is the velocity of the point $\boldsymbol{\eta}$ specified in the frame fixed to the undisturbed medium. We note that $\mathbf{V}$ has no component normal to the rotor plane. It is important to recognize that when we refer to $Q_{ij}|_{\boldsymbol{\eta}}$ we really mean that the components of the tensor Q_{ij} represented in coordinates that are instantaneously aligned with the rotating frame. Thus equation (17) provides the time derivative of $Q_{ij}|_{\mathbf{x}}$ in the stationary frame in terms of $Q_{ij}|_{\boldsymbol{\eta}}$ which is specified in the coordinates of the moving frame. Using the operator notation L_τ, the final emission-surface formulation may be written

$$\begin{aligned} 4\pi p'_Q(\mathbf{x},t) &= \frac{1}{c^2}\int \frac{1}{r}\hat{r}_i\hat{r}_j\left[L_\tau^2 Q_{ij}\right]_{ret} d\Sigma \\ &+ \frac{1}{c}\int \frac{1}{r^2}\left[3\hat{r}_i\hat{r}_j L_\tau Q_{ij} - L_\tau Q_{ii}\right]_{ret} d\Sigma \\ &+ \int \frac{1}{r^3}\left[3Q_{rr} - Q_{ii}\right]_{ret} d\Sigma\,. \qquad (18) \end{aligned}$$

Notice that the operator L_τ only operates on Q_{ij} because $\hat{r}_i$ and $\hat{r}_j$ do not depend upon t or τ. We refer to equation (18) as formulation Q2. Examining the definition (17) and equation (18), we realize that formulation Q2 is a singularity free expression for supersonic quadrupole noise. Note that equation (18) has second space and time derivatives of Q_{ij} as well as first space derivatives in the rotor plane. These quantities are available in the CFD postprocessor that is used to compute Q_{ij} for acoustic calculations. As it stands, formulation Q2 is valid for subsonic and supersonic quadrupole noise prediction for helicopter rotors in hover or forward flight. (Full details are given in reference 14.)

Formulation Q2 has been implemented in a demonstration code known as WOPWOP2+. WOPWOP2+ differs significantly from WOPWOP+[9–11] in that it uses an emission-surface formulation to compute thickness and loading noise, as well as the quadrupole noise. The construction of the emission surface and subsequent integration over the emission surface is performed using the method of marching cubes integration developed by Brentner.[15] In reference 14, it is shown that the subsonic (WOPWOP+) and the supersonic (WOPWOP2+) formulations give identical results when the quadrupole grid extent is the same. Ianniello[16] has also developed quadrupole noise prediction codes which utilize the far-field approach of Brentner[9,10] and he has developed a sophisticated emission-surface construction and integration scheme.[17]

We now present HSI noise calculations for a two-blade model-scale UH-1H rotor tested in hover with tip Mach numbers 0.88, 0.9, 0.925, and 0.95 (See reference 18 for test information). The quadrupole grid in these computations extends $1.86R$ beyond the blade tip for all the WOPWOP2+ calculations shown in figure 3. For comparison, we have also shown the signature predicted by WOPWOP+ which includes quadrupole sources only up to the sonic circle. The agreement of the WOPWOP2+ signature with the measured data is excellent and better than that of WOPWOP+ for each case. For the more intense cases ($M_H > 0.90$), the agreement of the WOPWOP2+ prediction with the measured acoustic pressure signature is not fully satisfactory because the WOPWOP2+ prediction overpredicts the negative peak pressure. This is apparent in figure 3 for the times between the WOPWOP+ and the WOPWOP2+ shock locations. Farassat and Brentner[14] identify this overprediction as numerical oscillation related to the bifurcation of the quadrupole source region at a critical source time.

3.2 FW–H equation revisited

One example of developing an alternative but equivalent source description has been the utilization of the FW–H equation on a permeable surface. In rotor noise prediction, the surface $f = 0$ has usually been assumed to be coincident with the rotor blade surface and impenetrable ($u_n = v_n$). A relaxation of that assumption is useful because it allow consideration of either conveniently placed fictitious surfaces or physical surfaces which permit flow through them.

For a permeable surface (fictitious or physical), equation (6) is the appropriate expression of the FW–H equation. It is clear from both the original Ffowcs Williams and Hawkings paper[1] and later work [19, Chapter 11, Sec 10] that Ffowcs Williams understood the value of utilizing equation (6) on a permeable surface. Recently di Francescantonio implemented this form of the FW–H equation for rotor noise prediction.[20] At nearly the same time, Brentner and Farassat demonstrated the relationship between the FW–H equation and the Kirchhoff equation for moving surfaces.[21] Many others have followed suit by quickly adopting the utilization of the FW–H equation on a permeable surface.[22–24]

One question to be considered is "What is the advantage of a fictitious surface that is not coincident with the physical body?" Although it may not be immediately obvious from equations (6) or (7), any physical acoustic sources enclosed by the $f = 0$ surface only contribute through the surface-source terms. Any physical sources of sound or propagation effects outside $f = 0$ only contribute through the volume source term. Hence, if we can enclose all physical sources inside $f = 0$ we have no contribution from the volume source—the quadrupole can be

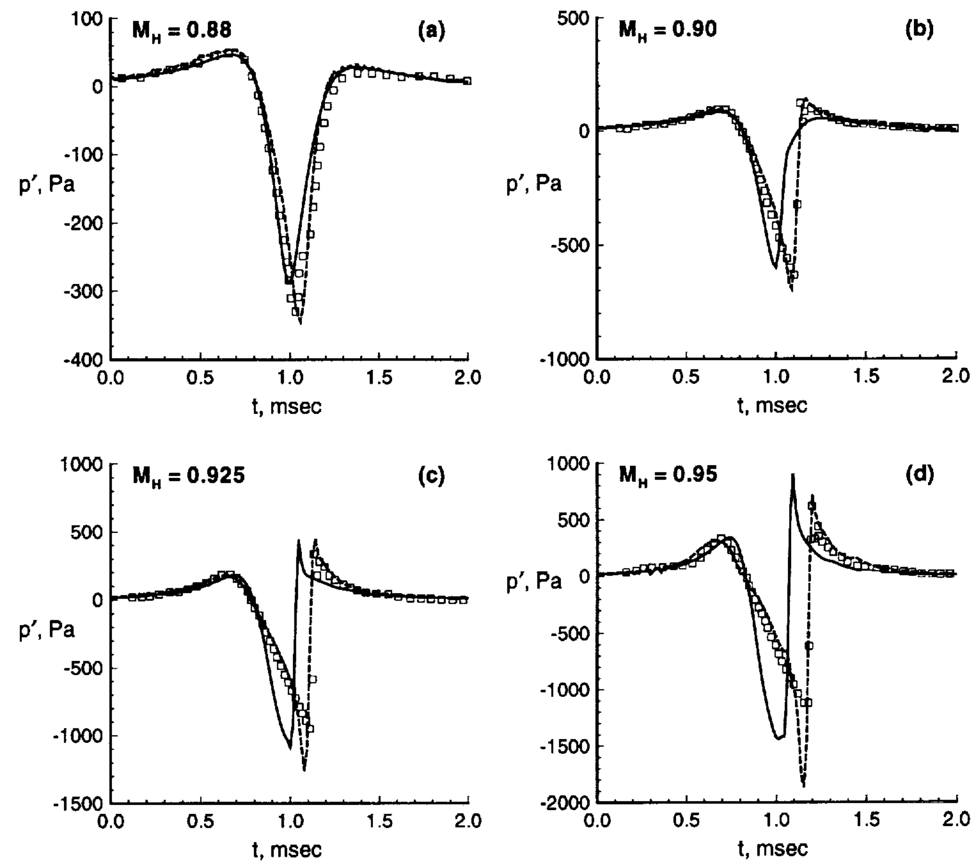

Figure 3. Comparison of WOPWOP+ (——) and WOPWOP2+ (- - -) predicted acoustic pressure with experimental data[18] (□) for hovering model UH-1H rotor. Quadrupole grid in WOPWOP+ prediction extended almost to sonic circle and in WOPWOP2+ predictions extended $1.86R$ beyond the rotor tip.

legitimately neglected. Without the quadrupole, a significant computational savings is realized because the volume integration is no longer required. Furthermore, the amount of flow-field data required for a surface integration is much less than for an integration of the the volume surrounded by the surface.

The enabling key to utilization of the FW–H equation on a permeable surface is the availability of an accurate flow-field description from CFD. Only recently has CFD matured point where it can provide sufficiently accurate, unsteady flow-field data on the integration surface. Even so, CFD computations for a rotor in forward flight are extremely demanding. Thus the coupling of the FW–H equation and CFD provides a mutually beneficial approach to computing the noise. The CFD computation only is needed in the acoustic source region—not all the way to the observer—and the FW–H equation provides an efficient method of predicting the sound field away from the source region. Through the utilization of the permeable surface formulation of the FW–H equation, the acoustic calculations can be made computationally efficient even for complicated, nonlinear acoustic sources.

To demonstrate the robustness and accuracy of the permeable surface application of the FW–H equation, a comparison between the predicted acoustic pressure and experiment for a hovering rotor is shown in figure 4. In the figure, the result for a WOPWOP+ prediction is also shown. The same CFD calculation was utilized for the input data all the predictions. Two permeable surface FW–H computations are show in figure 4: first, an integration surface coincident with the rotor blade to predict thickness and loading noise; and second, an integration surface located approximately 1.5 chordlengths away from the blade to predict the total noise. Note that the thickness noise predictions from WOPWOP+ and FW–H are identical and there is only a small difference in the predicted loading noise.

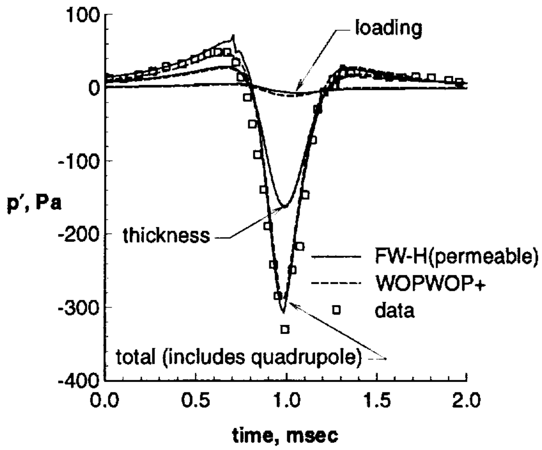

Figure 4. Comparison of noise components predicted by the FW–H/RKIR and WOPWOP+ codes for a hover UH-1H model rotor ($M_H = 0.88$, inplane observer $3.4R$ from rotor hub).

The total noise, which includes the effect of the quadrupole, is also in very close agreement even though the volume used in WOPWOP+ is not identical to the region enclosed in the FW–H permeable-surface integration.

3.3 Problems with the Kirchhoff formulation

The Kirchhoff formulation for moving surfaces is an alternative formulation that has been used for rotor noise prediction over the past decade. The Kirchhoff formulation gained rapid acceptance shortly after its publication by Farassat and Myers in 1988[25] precisely because it appeared to offer the same benefits just presented for the permeable-surface application of the FW–H equation. Nevertheless, recent work by Brentner and Farassat[21] and Singer et al.[26] have shown that the Kirchhoff formulation is unreliable for aeroacoustic problems in practice. This observation is sufficiently important that some explanation is desirable.

An embedding procedure similar to that used to derive the FW–H equation above was applied to the wave equation by Farassat and Myers to derive the Kirchhoff formulation for moving surfaces. The generalized wave equation—which is the governing equation for the Kirchhoff formulation—becomes

$$\begin{aligned}\Box^2 p'(\mathbf{x},t) &= -\left(\frac{\partial p'}{\partial t}\frac{M_n}{c} + \frac{\partial p'}{\partial n}\right)\delta(f) \\ &\quad - \frac{\partial}{\partial t}\left(p'\frac{M_n}{c}\delta(f)\right) - \frac{\partial}{\partial x_i}\left(p'\hat{n}_i\delta(f)\right) \\ &\equiv Q_{kir} \end{aligned} \qquad (19)$$

where $M_n = v_n/c$. In this equation p' must be compatible with the wave equation, hence, equation (19) is valid only in the region of the fluid in which the wave equation is the appropriate governing equation.

Through the utilization of the continuity and momentum equations we can rewrite the permeable surface form of the FW–H equation (6), as

$$\begin{aligned}\Box^2 p'(\mathbf{x},t) &= Q_{kir} + \frac{\bar{\partial}^2}{\partial x_i \partial x_j}[T_{ij}H(f)] \\ &+ \frac{\partial}{\partial t}[p' - c^2\rho']\frac{M_n}{c}\delta(f) + \frac{\partial}{\partial t}\left[(p' - c^2\rho')\frac{M_n}{c}\delta(f)\right] \\ &- \frac{\partial}{\partial x_j}[\rho u_i u_j]\hat{n}_i\delta(f) - \frac{\partial}{\partial x_i}[\rho u_i u_n \delta(f)]\ . \end{aligned} \qquad (20)$$

This form of the FW–H equation highlights the differences between the Kirchhoff formulation and the FW–H equation. Notice that all the additional source terms in equation (20) are second-order terms in perturbation quantities outside of the source region (i.e. $p' - c^2\rho' \ll 1$ and $\rho u_i u_j \ll 1$). For linear wave propagation, each of these terms would be identically zero and the Kirchhoff formulation and the FW–H equation would be in complete agreement. (A more detailed comparison and discussion are found in reference 21.)

To illustrate how the Kirchhoff formulation can give misleading results, consider a series of cylindrical integration surfaces which enclose a hovering rotor blade, as shown in figure 5. In figure 6, the acoustic pressure for an in-plane observer has been computed using both the FW–H equation and the Kirchhoff formulation for each of the integration surfaces.

Both methods agree reasonably well with the data when the integration surfaces are more than about 0.7 chords from the blade surface. The predicted acoustic pressure from the Kirchhoff computations for integration surfaces that are closer to the blade are unrealistic. The acoustic pressure predicted by the FW–H equation, however, is well behaved and is modified only by the fact that not all of the "quadrupole" noise source is included when the integration surface is too close to the blade and the volume source term in equation (6) has been neglected.

A second example illustrates another problem that can occur with the Kirchhoff formulation. In this

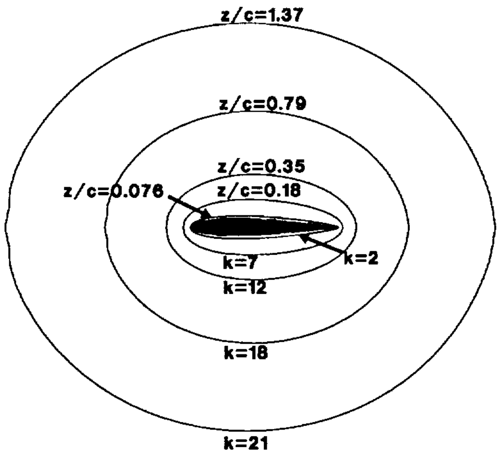

Figure 5. Concentric cylindrical integration surfaces used for noise computation for a hovering rotor.

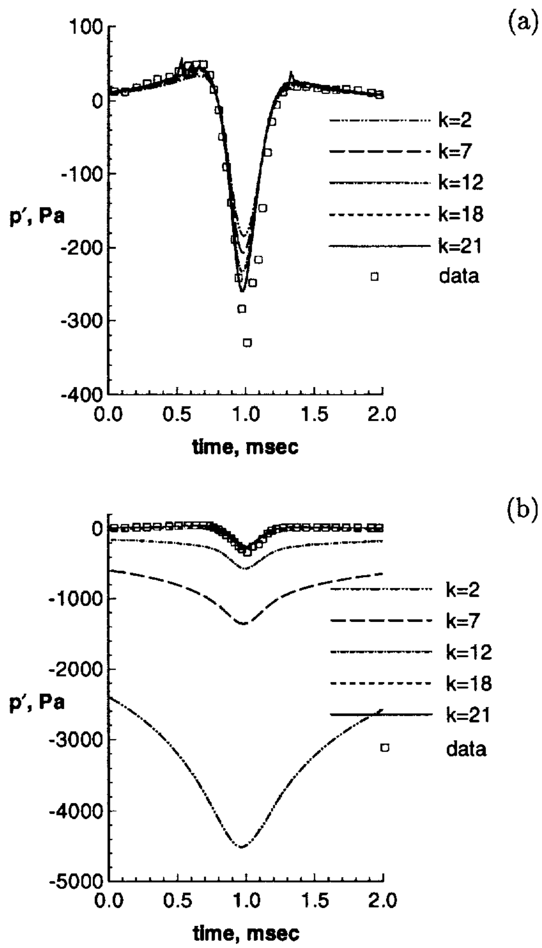

Figure 6. Predicted acoustic pressure for various integration surface locations for an observer located $3.4R$ from a UH-1H model rotor hovering at $M_H = 0.88$. The experimental data (□) is from reference 18. (a) FW–H prediction; (b) Kirchhoff prediction

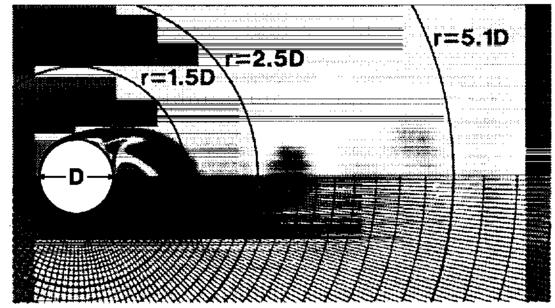

Figure 7. Vorticity field computed from CFD. FW–H integration surfaces are at $r = 0.5D$, $r = 1.5D$, $r = 2.5D$, and $r = 5.1D$

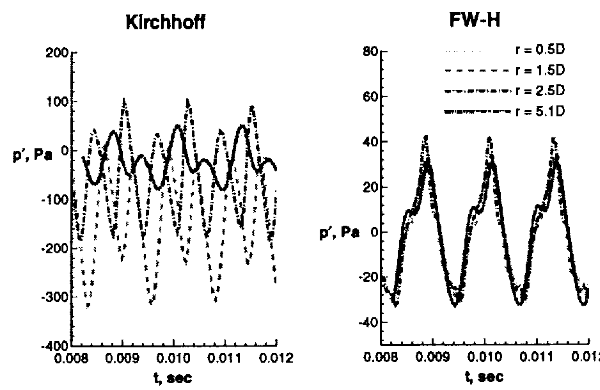

Figure 8. Acoustic signals computed for various integration surfaces that correspond to those indicated in Figure 7.

case, consider the viscous flow past a circular cylinder shown in figure 7. In this situation it is expected that the vortices shed by cylinder have a very small contribution to the sound produced, hence the acoustic signal should be relatively unaffected by the placement of the integration surface. Figure 8 shows that this is indeed the case for the FW–H computation, but the Kirchhoff computation does not even converge to a value but is entirely erroneous. This is significant for rotor noise prediction because rotor wakes inevitably must pass through the integration surface.

These two examples demonstrate numerically that the Kirchhoff formulation is not reliable for rotor noise prediction. Fortunately, from a computational point of view, there is very little difference between the methods. All of the computational advantages originally sought from the Kirchhoff method are available using the FW–H equation. Furthermore, all of the physical insight that the FW–H equation traditionally has provided is also still available.

4. Summary

In the last several years significant progress has been made in developing efficient quadrupole noise prediction formulations. Much of the work was motivated by the need for an efficient high-speed impulsive-noise prediction tool. The FW–H equation has proven to be a fruitful source of integral formulations and the desire to avoid the computation of the quadrupole noise altogether has lead to the utilization of the FW–H equation on permeable surfaces. The permeable-surface FW–H equation actually embodies all of HSI prediction methods because the full formulation still includes the quadrupole outside of the integration surface. It has also been demonstrated that the Kirchhoff formulation, while fine for acoustic problems, can be unreliable for aeroacoustics. Fortunately the FW–H equation is equally efficient and much more robust.

Although this paper has not dealt directly with rotorcraft aerodynamic computations, it should be pointed out that the acoustic formulations discussed require highly accurate solutions —both spatially and temporally—as input data. The aerodynamic calculations required for HSI noise in forward flight are extremely challenging. An accurate, first-principles, blade-vortex interaction computation is still beyond the ability of present day computers and CFD. Nevertheless, progress is being made and the acoustic propagation theory and codes will be up to the task.

References

1. Ffowcs Williams, J. E., and Hawkings, D. L., "Sound Generated by Turbulence and Surfaces in Arbitrary Motion," *Philosophical Transactions of the Royal Society*, Vol. A264, No. 1151, 1969, pp. 321–342.

2. Lighthill, M. J., "On Sound Generated Aerodynamically, I: General Theory," *Proceedings of the Royal Society*, Vol. A211, 1952, pp. 564–587.

3. Yu, Y. H., Caradonna, F. X., and Schmitz, F. H., "The Influence of the Transonic Flow Field on High-Speed Helicopter Impulsive Noise," Fourth European Rotorcraft and Powered Lift Aircraft Forum, 1978. Paper 58.

4. Hanson, D. B., and Fink, M. R., "The Importance of Quadrupole Sources in Prediction of Transonic Tip Speed Propeller Noise," *Journal of Sound and Vibration*, Vol. 62, No. 1, 1979, pp. 19–38.

5. Ffowcs Williams, J. E., "Sound Sources in Aerodynamics—Fact and Fiction," *AIAA Journal*, Vol. 20, No. 3, 1982, pp. 307–315.

6. Farassat, F., "Extension of Isom's Thickness Noise Formula to the Near Field," *Journal of Sound and Vibration*, Vol. 67, No. 2, 1979, pp. 280–281.

7. Farassat, F., "Theory of Noise Generation from Moving Bodies with an Application to Helicopter Rotors," NASA TR R-451, 1975.

8. Farassat, F., and Brentner, K. S., "The Uses and Abuses of the Acoustic Analogy in Helicopter Rotor Noise Prediction," *Journal of the American Helicopter Society*, Vol. 33, No. 1, Jan. 1988, pp. 29–36.

9. Brentner, K. S., and Holland, P. C., "An Efficient and Robust Method for Computing Quadrupole Noise," *Journal of the American Helicopter Society*, Vol. 42, No. 2, Apr. 1997, pp. 172–181.

10. Brentner, K. S., "An Efficient and Robust Method for Predicting Helicopter Rotor High-Speed Impulsive Noise," *Journal of Sound and Vibration*, Vol. 203, No. 1, 1997.

11. Brentner, K. S., "Prediction of Helicopter Discrete Frequency Rotor Noise—A Computer Program Incorporating Realistic Blade Motions and Advanced Acoustic Formulation," NASA TM 87721, Oct. 1986.

12. Visintainer, J. A., Marcolini, M. A., Burley, C. L., and Liu, S. R., "Acoustic Predictions Using Measured Pressures from a Model Rotor in the DNW," *Journal of the American Helicopter Society*, Vol. 38, No. 3, 1993, pp. 35–44.

13. Burley, C. L., and Tadghighi, H., "Importance of High Accuracy Blade Motion and Airloads Predictions in Acoustic Analysis," American Helicopter Society 50th Annual Forum, 1994.

14. Farassat, F., and Brentner, K. S., "Supersonic Quadrupole Noise Theory for High-Speed Helicopter Rotors," *Journal of Sound and Vibration*, Vol. 218, No. 3, 1998, pp. 481–500.

15. Brentner, K. S., "A New Algorithm for Computing Acoustic Integrals," *Proceedings of the IMACS 14th World Congress on Computational and Applied Mathematics*, Vol. 2, 1994, pp. 592–595.

16. Ianniello, S., "Quadrupole Noise Predictions Through the FW-H Equation," *AIAA Journal*, Vol. 37, No. 9, Sept. 1999, pp. 1048–1054.

17. Ianniello, S., "An Algorithm to Integrate the Ffowcs Williams–Hawings Equation on a Rotating, Supersonic Domain," AIAA 98-2378, June 1998.

18. Purcell, T. W., "CFD and Transonic Helicopter Sound," Fourteenth European Rotorcraft Forum, 1988. Paper 2.

19. Crighton, D. G., Dowling, A. P., Ffowcs Williams, J. E., Heckl, M., and Leppington, F. G., *Modern Methods in Analytical Acoustics: Lecture Notes*, Springer-Verlag, London, 1992.

20. di Francescantonio, P., "A New Boundary Integral Formulation for the Prediction of Sound Radiation," *Journal of Sound and Vibration*, Vol. 202, No. 4, 1997, pp. 491–509.

21. Brentner, K. S., and Farassat, F., "An Analytical Comparison of the Acoustic Analogy and Kirchhoff Formulation for Moving Surfaces," *AIAA Journal*, Vol. 36, No. 8, Aug. 1998, pp. 1379–1386.

22. Pilon, A. R., and Lyrintzis, A. S., "Integral Methods for Computational Aeroacoustics," AIAA Paper 97-0020, Jan. 1997.

23. Strawn, R. C., Duque, E. P. N., and Ahmad, J., "Rotorcraft Aeroacoustics Computations with Overset-Grid CFD Methods," *Journal of the American Helicopter Society*, Vol. 44, No. 2, Apr. 1999, pp. 132–140.

24. Prieur, J., and Rahier, G., "Comparison of Ffowcs Williams–Hawkings and Kirchhoff Rotor Noise Calculations," AIAA Paper 98-2376, 1998.

25. Farassat, F., and Myers, M. K., "Extension of Kirchhoff's Formula to Radiation from Moving Surfaces," *Journal of Sound and Vibration*, Vol. 123, No. 3, 1988, pp. 451–461.

26. Singer, B. A., Brentner, K. S., Lockard, D. P., and Lilley, G. M., "Simulation of Acoustic Scattering from a Trailing Edge," AIAA Paper 99-0231, Jan. 1999.